ChemComm

COMMUNICATION

View Article Online
View Journal

Cite this: DOI: 10.1039/d2cc00853j

Received 10th February 2022,
Accepted 21st March 2022

DOI: 10.1039/d2cc00853j

rsc.li/chemcomm

Electrocatalytic reduction of nitrate by *in situ* generated cobalt nanoparticles†

Moumita Ghosh, Maha Ibrar and Jeremy M. Smith *

The cobalt pyridinophane complex $[Co(^{H}N4)Cl_2]^+$ ($^{H}N4$ = 3,7-diaza-1,5(2,6)-dipyridinacyclooctaphane) is converted under catalytic conditions to an electrode-adsorbed species. Aqueous Co^{2+} solutions similarly deposit a species under these conditions. Surface characterization reveals the formation of Co nanoparticles. These nanoparticles are active in the electrocatalytic redution of aqueous nitrate.

The industrial Haber–Bosch process radically altered the world's food production dynamics by dramatically increasing the supply of ammonia-based fertilizers.[1] About 80% of Haber–Bosch produced NH_3 is used for fertilizers, with the resulting agricultural output estimated to support half the world's population.[2] While 100 Tg NH_3 is used as fertilizer each year, only a fifth of the applied nitrogen is consumed as food protein by humans and livestock.[1] The rest is oxidized by soil bacteria to an assortment of nitrogen oxides. Among these is the highly soluble nitrate oxyanion, which runs off fields into nearby waterbodies.[3] These nitrate anions stimulate algal blooms, leading to eutrophication and ultimately the formation of aquatic "dead zones",[4,5] which are associated with significant economic and environmental consequences.[4,6]

Denitrification is typically achieved either through physical separation or by biological processes, presenting an opportunity to develop new methods of converting nitrate into value-added products.[7] Among these is electrocatalytic reduction, which in principle allows for the selective conversion of aqueous nitrate through an applied potential. Although thermodynamically favorable (*e.g.*, E^0 = +0.44 V *vs.* NHE at pH 6.0 for the reduction to NH_4^+), nitrate reduction is challenging for two main reasons. Firstly, the delocalized electronic structure of nitrate hinders effective binding to catalysts.[8] Indeed, nitrate is often outcompeted by other ions present in aqueous media, such as halides, CO_3^{2-}, and PO_4^{3-}.[9,10] Secondly, since many of its reduced species are stable,[11] product selectivity is a significant challenge for electrocatalytic nitrate reduction.

Molecular electrocatalysts have the advantage being highly tunable, typically through ligand modification. In addition, the well-defined nature of these catalysts makes them better suited to mechanistic interrogation. However, in some cases, molecular complexes have been observed to decompose under reductive conditions, generating surface-adsorbed nanoparticles that are the catalytically active species.[12,13]

We previously investigated the complex $[Co(DIM)Br_2]^+$ (2,3-dimethyl-1,4,8,11-tetraazacyclotetradeca-1,3-diene), which reduces nitrate with high faradaic efficiency over a wide pH range.[10] Mechanistic investigations reveal the critical role of the macrocycle, whose structural flexibility facilitates the binding of nitrate, specifically by creating a *cis*-divacant geometry at the metal. This insight led us to target the cobalt pyridinophane complex $[Co(^{H}N4)Cl_2]^+$ ($^{H}N4$ = 3,7-diaza-1,5(2,6)-dipyridinacyclooctaphane) (Fig. 1) as a nitrate reduction electrocatalyst. A notable feature of pyridinophane macrocycles is their ability to enforce the *cis*-divacant geometry that facilitates the bidentate binding of nitrate. In addition, the amines of the macrocycle are appropriately placed to shuttle the protons required for nitrate reduction.

Here, we report investigations into the electrocatalytic activity of $[Co(^{H}N4)Cl_2]^+$ towards the reduction of aqueous nitrate. Unexpectedly, the complex is unstable under catalytic conditions, decomposing to provide a surface-supported catalyst for electrocatalytic nitrate reduction. Similar reduction of aqueous cobalt

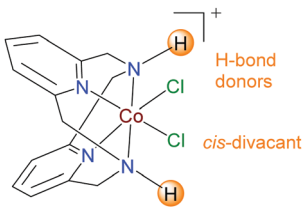

Fig. 1 Structure of $[Co^{III}(^{H}N4)Cl_2]^+$.

Department of Chemistry, Indiana University, 800 E. Kirkwood Ave., Bloomington, IN 47401, USA. E-mail: smith962@indiana.edu

† Electronic supplementary information (ESI) available. See DOI: 10.1039/d2cc00853j

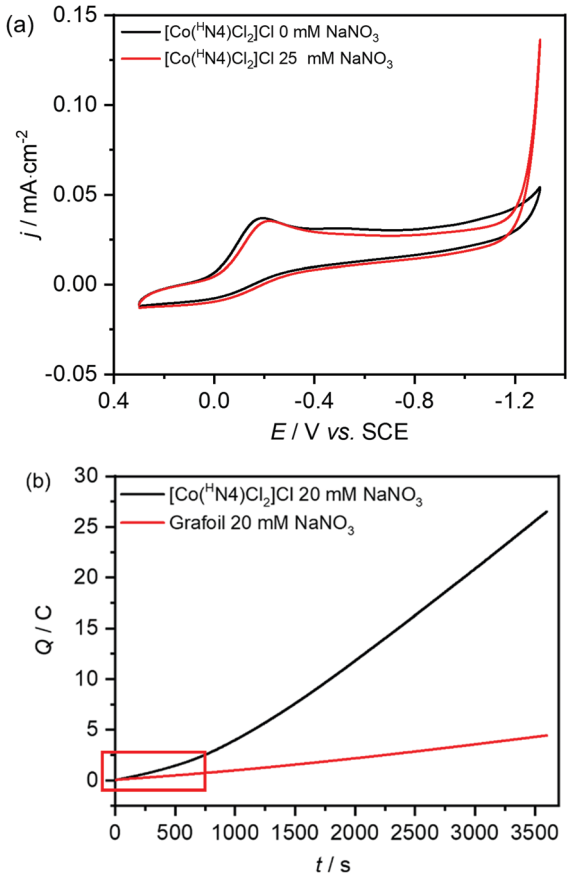

Fig. 2 (a) Cyclic voltammograms of 1 mM $[Co(^{H}N4)Cl_2]^+$ in 0.1 M Na_2SO_4, pH 6.0 at glassy carbon working electrode (black) and with 25 mM $NaNO_3$ (red), scan rate 25 mV s^{-1}; (b) charge passed during 1 h CPE of 1 mM $[Co(^{H}N4)Cl_2]^+$ at −1.31 V *vs.* SCE (20 mM $NaNO_3$, 0.1 M Na_2SO_4, initial pH 5.3, Grafoil working electrode). The induction period is highlighted.

solutions provides cobalt nanoparticles that are catalytically active for nitrate reduction.

The CV of aqueous $[Co(^{H}N4)Cl_2]^+$ (pH 6.00, 0.1 M Na_2SO_4) shows an irreversible reductive process with $E_{p,c}$ = −0.21 V *vs.* SCE (Fig. 2(a)) that we attribute to the Co(III)/Co(II) couple. No processes are observed at more cathodic potentials.

Despite the lack of additional reductive processes in the absence of substrate, current enhancement is observed when the CV of aqueous $[Co(^{H}N4)Cl_2]^+$ is measured in the presence of nitrate. Specifically, a new wave with onset potential ∼ −1.1 V *vs.* SCE is observed in the CV of $[Co(^{H}N4)Cl_2]^+$ and 25 mM $NaNO_3$ (Fig. 2(a)). The current increases with increasing $NaNO_3$ concentration, as expected for the electrocatalytic reduction of nitrate (Fig. S3, ESI†). Further evidence for electrocatalytic nitrate reduction comes from a controlled potential electrolysis (CPE) experiment. Product characterization following 1 h CPE at −1.31 V *vs.* SCE (Fig. 2(b)) reveals the formation of ammonium with modest faradaic efficiency (68 ± 5%). No hydroxylamine or nitrite is detected.

It is notable that the CPE experiment is associated with an induction period (Fig. 2(b), highlighted) suggesting that $[Co(^{H}N4)Cl_2]^+$ serves as a precursor to a catalytically active species. Specifically, the initial rate of charge consumption is slow, but shows a clear increase over the first ∼750 s. At the same time, the colour of the electrolysis solution changes from pale purple to yellow brown (Fig. S5, ESI†), strongly suggesting the instability of $[Co(^{H}N4)Cl_2]^+$ under the electrocatalytic conditions (Fig. S11, ESI†). Following this induction period, the rate of charge consumption remains constant.

A rinse test of the working electrode reveals that $[Co(^{H}N4)Cl_2]^+$ decomposition provides a catalytically active species on the electrode surface. Specifically, following a CPE experiment, the working electrode was thoroughly rinsed to remove water-soluble species and then immersed in a fresh electrolyte solution containing 20 mM $NaNO_3$ substrate but no $[Co(^{H}N4)Cl_2]^+$. The resulting CV reveals a catalytic current having onset potential −0.91 V *vs.* SCE (Fig. S4, ESI†), consistent with the formation of a surface-adsorbed nitrate reduction electrocatalyst. It is notable that this onset is observed at a potential that is ∼0.2 V more anodic than observed for electrocatalysis with $[Co(^{H}N4)Cl_2]^+$, consistent with the complex being a precursor to the true catalyst. The less cathodic potential required for $[Co(^{H}N4)Cl_2]^+$ decomposition also suggests that the complex is unlikely to play any role in nitrate reduction and that the surface-adsorbed species is solely responsible for the observed electrocatalytic activity. Indeed, a CPE experiment of the surface-adsorbed species in the presence of $NaNO_3$ reveals the formation of ammonium with 90 ± 5% faradaic efficiency (Fig. S13, ESI†), along with H_2 in 8.5% faradaic efficiency. Control experiments establish that the cathodic potential is critical for the decomposition of $[Co(^{H}N4)Cl_2]^+$ (Fig. S6, ESI†).

X-Ray photoelectron spectroscopy (XPS) of the working electrode following CPE provides insight into the nature of the surface-adsorbed species. Most notably, high resolution XPS exhibits Co 2p peaks at 781.04 eV and 797.01 eV that are absent for a fresh electrode (Fig. 4).

Hypothesizing that reduced $[Co(^{H}N4)Cl_2]^+$ serves as a source of aqueous cobalt ions, which are in turn reduced to the surface-adsorbed electrocatalyst, we investigated aqueous Co^{2+} as an electrocatalyst precursor. It has been previously established that morphologically unstable metallic cobalt nanoparticles can be electrodeposited from aqueous $CoCl_2$ solutions.[14] Deposition of metallic cobalt commences at −0.81 V *vs.* SCE, with a rapid increase in current at more cathodic potentials attributed to nucleation.[14] We observe similar behavior in the CV of an aqueous cobalt solution with a glassy carbon working electrode (1 mM $CoCl_2$, 0.1 M Na_2SO_4) (Fig. 3). Specifically, on the cathodic scan, a rapid increase in current occurs at −0.86 V *vs.* SCE, consistent with the deposition of cobalt on the electrode surface. This is supported by a broad anodic current enhancement at −0.18 V *vs.* SCE on the anodic scan, as expected for the electrochemical stripping of electrode-deposited material.

Importantly, the surface deposited cobalt nanoparticles are active towards the electrocatalytic reduction of aqueous nitrate. A catalytic current with onset potential ∼ −0.9 V *vs.* SCE is observed in the presence of 25 mM $NaNO_3$ substrate (Fig. 3). This is the same onset potential as observed for the surface-

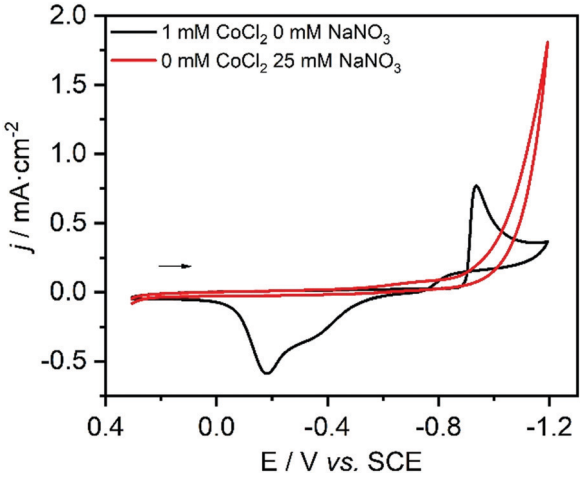

Fig. 3 Cyclic voltammograms of 1 mM $CoCl_2{\cdot}6H_2O$ in 0.1 M Na_2SO_4, pH 6.0 at glassy carbon working electrode (black). The same electrode was immersed in a fresh 0.1 M Na_2SO_4 solution, 25 mM $NaNO_3$ (red). Scan rate 25 mV s^{-1} for both CVs.

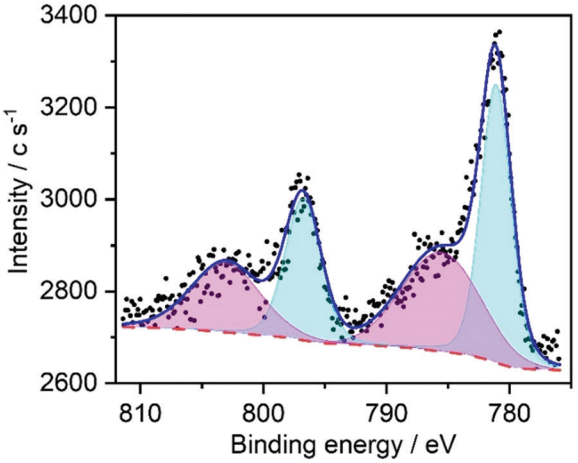

Fig. 4 High-resolution Co 2p XPS spectrum of the Grafoil electrode after CPE of 1 mM $[Co(^{H}N4)Cl_2]^+$ at −1.31 V *vs.* SCE for 2 h (0.1 M Na_2SO_4). The measured signal is in black, the overall fit manifold in blue, and the fit peaks in cyan and magenta.

deposited material that is formed from the decomposition of $[Co(^{H}N4)Cl_2]^+$. A rinse test confirms that the electrodeposited material is responsible for nitrate reduction (Fig. S8, ESI†). Aqueous solutions of $CoBr_2$ similarly form an electrodeposit in the absence of any nitrate. This material is also active for the electrocatalytic reduction of nitrate (Fig. S14, ESI†), indicating that chloride plays no role in active catalyst formation.

XPS following CPE confirms the deposition of cobalt on the working electrode surface. A survey spectrum reveals both Co 2p and N 1s signals, with the source of the latter attributed to the nitrate anion. The high-resolution Co 2p spectrum displays the $2p_{3/2}$ and $2p_{1/2}$ doublets at 781.04 eV and 797.01 eV respectively (Fig. S7, ESI†).[15]

Scanning electron microscopy (SEM) images of flexible graphitic carbon (Grafoil) working electrodes following CPE with $[Co(^{H}N4)Cl_2]^+$ in the absence (Fig. 5(a)) and presence (Fig. 5(b)) of nitrate substrate show the formation of cobalt nanoparticles on the electrode surface. Similarly, SEM reveals the formation of nanoparticles when $CoCl_2$ is used as the cobalt source (Fig. S17, ESI†). The SEM images reveal a diversity of morphologies, consistent with earlier reports on the morphological instability of electrodeposited cobalt nanoparticles on glassy carbon.[16] This suggests that the morphology of the nanoparticles is not critical for their electrocatalytic activity. Consistent with the XPS results, energy dispersive X-ray spectroscopy (EDS) analysis of the electrode surface following CPE reveals significant amounts of cobalt for both $CoCl_2$ and $[Co(^{H}N4)Cl_2]^+$ (Table S1, ESI†).

In this work, we have shown the homogeneous complex $[Co(^{H}N4)Cl_2]^+$ decomposes under reducing conditions to form a surface-adsorbed species that is active for the efficient electrocatalytic reduction of aqueous nitrate. Similar reduction of aqueous Co^{2+} solutions create a surface-adsorbed nanoparticle cobalt electrocatalyst for the reduction of nitrate to ammonium.

There has been a growing interest in the development of the electrocatalytic methods for the reduction of aqueous nitrate

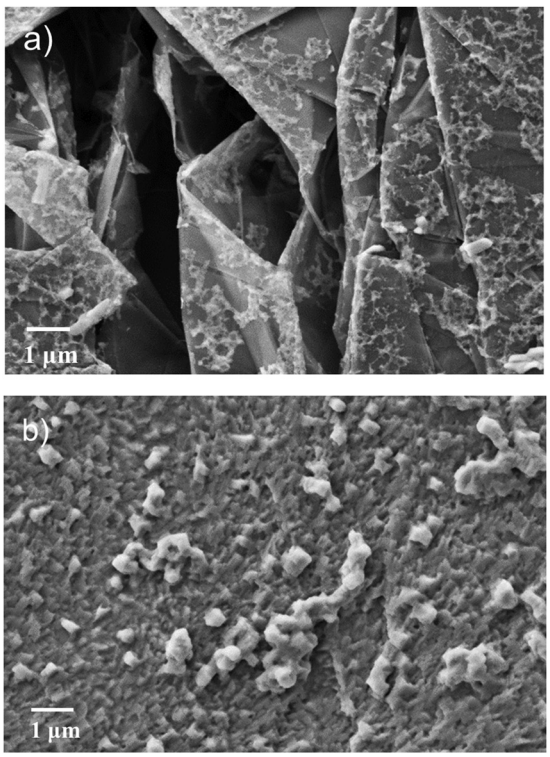

Fig. 5 (a) SEM image of cobalt deposits on the Grafoil electrode after CPE at −1.31 V *vs.* SCE for 1 h without any nitrate; (b) SEM image of cobalt deposits on the Grafoil electrode after CPE at −1.31 V *vs.* SCE for 1 h with 20 mM nitrate (0.1 M Na_2SO_4, 1 mM $[Co(^{H}N4)Cl_2]^+$ for both experiments).

and nitrite.[17–22] As has been observed for some other electrochemical transformations (*e.g.* water oxidation[23,24] and reduction[12,13]), our results demonstrate that the decomposition of molecular complexes to catalytically active nanomaterials also needs to be considered in the context of the electrocatalytic reduction of nitrogen oxyanions. Indeed, certain transition

metal nanoparticles have been reported to be active in the electrocatalytic reduction of nitrate.[25–27]

We gratefully acknowledge funding from the NSF (CHE-2102442). We thank Jun Chen and Nayana Christudas Beena for experimental assistance.

Conflicts of interest

There are no conflicts to declare.

Notes and references

1 V. Smil, *World Agric.*, 2011, **2**, 9–13.
2 J. W. Erisman, M. A. Sutton, J. Galloway, Z. Klimont and W. Winiwarter, *Nat. Geosci.*, 2008, **1**, 636–639.
3 S. Matassa, D. J. Batstone, T. Hülsen, J. Schnoor and W. Verstraete, *Environ. Sci. Technol.*, 2015, **49**, 5247–5254.
4 R. Vaquer-Sunyer and C. M. Duarte, *Proc. Natl. Acad. Sci. U. S. A.*, 2008, **105**, 15452–15457.
5 J. P. Tanzer, C. Lawrence, A. Gonzales, A. Roxburgh and T. P. Gamblin, *Living Blue Planet Report: Species, Habitats and Human Well-Being*, WWF: Gland, Switzerland, 2015.
6 M. D. Smith, A. Oglend, A. J. Kirkpatrick, F. Asche, L. S. Bennear, J. K. Craig and J. M. Nance, *Proc. Natl. Acad. Sci. U. S. A.*, 2017, **114**, 1512–1517.
7 V. B. D. Jensen, J. L. Seidel and C. Gorman, *Drinking Water Treatment for Nitrate*, University of California, Davis, 2012.
8 L. Taniguchi, N. Nakashima and K. Yasukouchi, *J. Chem. Soc., Chem. Commun.*, 1986, 1814–1815.
9 S. E. Braley, D. C. Ashley, E. Jakubikova and J. M. Smith, *Chem. Commun.*, 2020, **56**, 603–606.
10 S. Xu, D. C. Ashley, H.-Y. Kwon, G. R. Ware, C.-H. Chen, Y. Losovyj, X. Gao, E. Jakubikova and J. M. Smith, *Chem. Sci.*, 2018, **9**, 4950–4958.
11 V. Rosca, M. Duca, M. T. de Groot and M. T. M. Koper, *Chem. Rev.*, 2009, **109**, 2209–2244.
12 N. Kaeffer, A. Morozan, J. Fize, E. Martinez, L. Guetaz and V. Artero, *ACS Catal.*, 2016, **6**, 3727–3737.
13 E. Anxolabéhère-Mallart, C. Costentin, M. Fournier, S. Nowak, M. Robert and J.-M. Savéant, *J. Am. Chem. Soc.*, 2012, **134**, 6104–6107.
14 C. Q. Cui, S. P. Jiang and A. C. C. Tseung, *J. Electrochem. Soc.*, 1990, **137**, 3418–3423.
15 C. D. Wagner, *The NIST X-Ray Photoelectron Spectroscopy (XPS) Database*, Washington, DC, 1991.
16 S. Fletcher, C. S. Halliday, D. Gates, M. Westcott, T. Lwin and G. Nelson, *J. Electroanal. Chem. Interfacial Electrochem.*, 1983, **159**, 267–285.
17 R. Jia, Y. Wang, C. Wang, Y. Ling, Y. Yu and B. Zhang, *ACS Catal.*, 2020, **10**, 3533–3540.
18 Z. Wang, D. Richards and N. Singh, *Catal. Sci. Technol.*, 2021, **11**, 705–725.
19 Y. Wang, W. Zhou, R. Jia, Y. Yu and B. Zhang, *Angew. Chem., Int. Ed.*, 2020, **59**, 5350–5354.
20 Y. Wang, A. Xu, Z. Wang, L. Huang, J. Li, F. Li, J. Wicks, M. Luo, D.-H. Nam, C.-S. Tan, Y. Ding, J. Wu, Y. Lum, C.-T. Dinh, D. Sinton, G. Zheng and E. H. Sargent, *J. Am. Chem. Soc.*, 2020, **142**, 5702–5708.
21 Y. Huang, J. Long, Y. Wang, N. Meng, Y. Yu, S. Lu, J. Xiao and B. Zhang, *ACS Appl. Mater. Interfaces*, 2021, **13**, 54967–54973.
22 P. H. van Langevelde, I. Katsounaros and M. T. M. Koper, *Joule*, 2021, **5**, 290–294.
23 J. J. Stracke and R. G. Finke, *J. Am. Chem. Soc.*, 2011, **133**, 14872–14875.
24 R. K. Hocking, R. Brimblecombe, L.-Y. Chang, A. Singh, M. H. Cheah, C. Glover, W. H. Casey and L. Spiccia, *Nat. Chem.*, 2011, **3**, 461–466.
25 Y. Lan, J. Chen, H. Zhang, W.-X. Zhang and J. Yang, *J. Mater. Chem.*, 2020, **8**, 15853–15863.
26 Z. A. Jonoush, A. Rezaee and A. Ghaffarinejad, *J. Cleaner Prod.*, 2020, **242**, 118569.
27 W. Siriwatcharapiboon, Y. Kwon, J. Yang, R. L. Chantry, Z. Li, S. L. Horswell and M. T. M. Koper, *ChemElectroChem*, 2014, **1**, 172–179.

